

Probing Decoherence with Electromagnetically Induced Transparency in Superconductive Quantum Circuits

K. V. R. M. Murali, D. S. Crankshaw, and T. P. Orlando

*Department of Electrical Engineering and Computer Science
Massachusetts Institute of Technology, Cambridge MA 02139*

Z. Dutton

National Institute of Standards & Technology, Electron and Optical Division, Gaithersburg MD 20899-8410

W. D. Oliver

MIT Lincoln Laboratory, 244 Wood Street, Lexington, MA 02420

(Dated: October 31, 2018)

Superconductive quantum circuits (SQCs) comprise quantized energy levels that may be coupled *via* microwave electromagnetic fields. Described in this way, one may draw a close analogy to atoms with internal (electronic) levels coupled by laser light fields. In this Letter, we present a superconductive analog to electromagnetically induced transparency (S-EIT) that utilizes SQC designs of present day experimental consideration. We discuss how S-EIT can be used to establish macroscopic coherence in such systems and, thereby, utilized as a sensitive probe of decoherence.

PACS numbers: 42.50.Gy

Superconductive quantum circuits (SQCs) comprising mesoscopic Josephson junctions can exhibit quantum coherence amongst their macroscopically large degrees of freedom [1]. They exhibit quantized flux and/or charge states depending on their fabrication parameters, and the resultant quantized energy levels are analogous to the quantized internal levels of an atom. Spectroscopy, Rabi oscillation, and Ramsey interferometry experiments have demonstrated that SQCs behave as “artificial atoms” under carefully controlled conditions [2, 3, 4, 5, 6, 7, 8, 9]. This Letter extends the SQC-atom analogy to another quantum optical effect associated with atoms: electromagnetically induced transparency (EIT) [10, 11]. We propose the demonstration of microwave transparency using a superconductive analog to EIT (denoted S-EIT) in a superconductive circuit exhibiting two meta-stable states (e.g., a qubit) and a third, shorter-lived state (e.g., the readout state). We show that driving coherent microwave transitions between the qubit states and the readout state is a demonstration of S-EIT. We further propose a means to use S-EIT to experimentally probe the qubit decoherence rate in a sensitive manner. The philosophy is similar to that in Ref. 12, where it was proposed to use EIT to measure phase diffusion in atomic Bose-Einstein condensates.

The three-level Λ system illustrated in Fig. 1a is a standard energy level structure utilized in EIT [10, 11]. It comprises two meta-stable states $|1\rangle$ and $|2\rangle$, each of which may be coupled to a third excited state $|3\rangle$. In atoms, the meta-stable states are typically hyperfine or Zeeman levels, while state $|3\rangle$ is an excited electronic state that may spontaneously decay at a relatively fast rate Γ_3 . In an atomic EIT scheme, a resonant “probe” laser couples the $|1\rangle \leftrightarrow |3\rangle$ transition, and a “control” laser couples the $|2\rangle \leftrightarrow |3\rangle$ transition. The transition coupling strengths are characterized by their Rabi fre-

quencies $\Omega_{j3} \equiv -\mathbf{d}_{j3} \cdot \mathbf{E}_{j3}$ for $j = 1, 2$ respectively, where \mathbf{d}_{j3} are the dipole matrix elements and \mathbf{E}_{j3} are the slowly varying envelopes of the electric fields. For particular Rabi frequencies Ω_{j3} , the probe and control fields are effectively decoupled from the atoms by a destructive quantum interference between the states of the two driven transitions. The result is probe and control field transparency [10, 11]. In more recent experiments, ultra-slow light propagation due to EIT-based refractive index modifications in atomic clouds have also been demonstrated [13, 14, 15].

SQCs have also been demonstrated to exhibit Λ -like energy level structures [7, 16, 17, 18]. One example is the persistent-current (PC) qubit, a superconductive loop interrupted by two Josephson junctions of equal size and a third junction scaled smaller in area by the factor $\alpha < 1$ (Fig. 1b) [19, 20]. Its dynamics are described by the Hamiltonian

$$\mathcal{H}_{pc} = \frac{1}{2}C \left(\frac{\Phi_0}{2\pi} \right)^2 (\dot{\varphi}_p^2 + (1 + 2\alpha)\dot{\varphi}_m^2) + E_J [2 + \alpha - 2 \cos \varphi_p \cos \varphi_m - \alpha \cos(2\pi f + 2\varphi_m)], \quad (1)$$

in which C is the capacitance of the larger junctions, $\varphi_{p,m} \equiv (\varphi_1 \pm \varphi_2)/2$, φ_i is the gauge-invariant phase across the larger junctions $i = \{1, 2\}$, E_J is the Josephson coupling energy, and f is the magnetic flux through the loop in units of the flux quantum Φ_0 . The second term in Eq. (1) defines the magnetic-flux-dependent qubit potential landscape. For flux biases near one-half of a flux quantum, $f \approx 1/2$, the potential may be approximated by a double-well potential, with each well corresponding to a distinct, stable, classical state of the electric current, i.e., left or right circulation through the loop. In turn, each current state has a net magnetization of oppo-

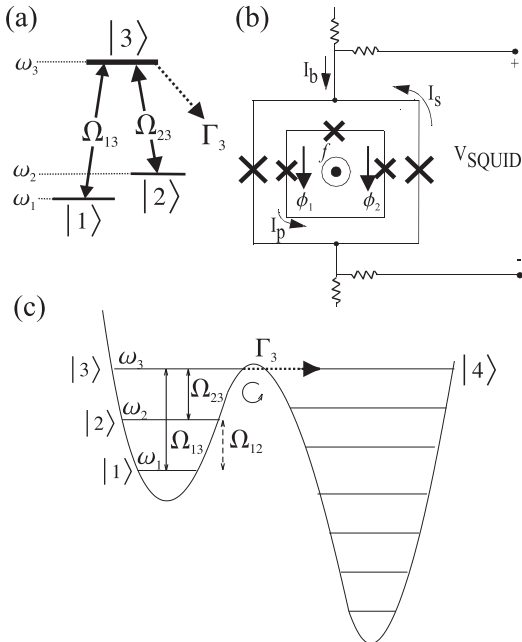


FIG. 1: (a) Energy level diagram of a three-level Λ system. EIT can occur in atoms possessing two long-lived states $|1\rangle, |2\rangle$, each of which is coupled *via* resonant laser light fields to a radiatively decaying state $|3\rangle$. State $|3\rangle$ can feed back into $|1\rangle, |2\rangle$ and/or decay into levels outside the Λ configuration. (b) Circuit schematic of the PC qubit and its readout SQUID. (c) Schematic energy level diagram for a three-level superconducting quantum circuit. For our parameters we calculate $\omega_2 - \omega_1 = (2\pi) 36$ GHz and $\omega_3 - \omega_2 = (2\pi) 32$ GHz. The simulated matrix elements are $\langle p | \sin(2\pi f + 2\phi_m) | q \rangle$ for $(p, q) = (1, 2), (2, 3)$, and $(1, 3)$ are, respectively, 0.0704, -0.125, 0.0158.

site direction that is measurable using a dc SQUID [19]. As a quantum object, the potential wells exhibit quantized energy levels corresponding to the quantum states of the macroscopic circulating current [16, 18]. These levels may be coupled using microwave radiation [4, 17], and their quantum coherence has been experimentally demonstrated [8]. Note that for this system, the terms “population” and “occupation probability” are used synonymously.

Tuning the flux bias away from $f = 1/2$ results in the asymmetric double-well potential illustrated in Fig. 1c. The three states in the left well constitute the superconductive analog to the atomic Λ system. States $|1\rangle$ and $|2\rangle$ are “meta-stable states,” with a tunneling and coherence time much longer than the excited “readout” state $|3\rangle$. State $|3\rangle$ has weakly-coupled intra-well transitions, but has a strong inter-well transition when tuned on resonance with state $|4\rangle$ [16, 17, 18]. Using tight-binding models with experimental PC qubit parameters [17, 18, 19] at a flux bias $f=0.5041$, we estimate the tunneling times from states $|1\rangle, |2\rangle$, and $|3\rangle$ to the right well are $1/\Gamma_1 \approx 1$ ms, $1/\Gamma_2 \approx 1$ μ s, and $1/\Gamma_3 \approx 1$ ns respectively. Thus, a particle reaching state $|3\rangle$ will tend

to tunnel quickly to state $|4\rangle$, and this event results in a switching of the circulating current that may be detected using a fast-measurement scheme. Alternatively, one may detune states $|3\rangle$ and $|4\rangle$, and then apply a resonant π -pulse to transfer the population from state $|3\rangle$ to $|4\rangle$; since the states are now off-resonance, the relaxation rate back to the left well is reduced and a slower detection scheme may be used. We note that a single-junction qubit [7] shares this property, since the right well in Fig. 1c is effectively replaced by a quasi-continuum of states, and transitions out of the left well will not return.

Transitions between the quantized levels are driven by resonant microwave-frequency magnetic fields. Assuming the Rabi frequencies Ω_{ij} to be much smaller than all level spacings $|\omega_{kl}| \equiv |\omega_k - \omega_l|$, the system-field interaction may be written within the rotating wave approximation (RWA)[21],

$$\mathcal{H}_{int}^{(RWA)} = \frac{\hbar}{2} \begin{bmatrix} 0 & \Omega_{12}^* & \Omega_{13}^* \\ \Omega_{12} & 0 & \Omega_{23}^* \\ \Omega_{13} & \Omega_{23} & -i\Gamma_3 \end{bmatrix}, \quad (2)$$

in which the decay from state $|3\rangle$ is treated phenomenologically as a non-Hermitian matrix element [21, 22]. For small microwave perturbations of amplitude f_Δ , the associated Rabi frequencies are given by $\Omega_{pq} = f_\Delta \langle p | \sin(2\pi f + 2\phi_m) | q \rangle$; numerical simulations of the matrix elements using PC qubit parameters are consistent with recent experimental results (see caption Fig. 1c) [16, 17, 18]. In general, all three intra-well transitions are allowed in SQCs. For example, consider states $|1\rangle$ and $|2\rangle$ to be a qubit that is prepared in an arbitrary superposition state $|\Psi\rangle = c_1|1\rangle + c_2|2\rangle$ by temporarily driving the Ω_{12} transition. Then, by applying a probe field, the population of state $|1\rangle$ may be read out through a transition to state $|3\rangle$ followed by a rapid escape to the right well [7]. In this case, both the preparation and readout transitions were allowed and absorptive.

One may achieve S-EIT in a superconductive Λ system that is prepared in state $|\Psi\rangle = c_1|1\rangle + c_2|2\rangle$, by simultaneously and solely applying the microwave fields Ω_{13} and Ω_{23} such that

$$\frac{\Omega_{13}}{\Omega_{23}} = -\frac{c_2}{c_1}. \quad (3)$$

Under this condition (with $\Omega_{12} = 0$), the state $|\Psi\rangle$ is an eigenstate of $\mathcal{H}_{int}^{(RWA)}$ in Eq. (2) with eigenvalue zero, and the SQC becomes transparent to the microwave fields. As in conventional EIT, the amplitudes for the two absorption transitions into $|3\rangle$ have equal and opposite probability amplitudes, leading to a destructive quantum interference. Thus, in the absence of decoherence, preparing the qubit in state $|\Psi\rangle$ with an ideal preparation (Ω_{12}) field and subsequently applying ideal probe (Ω_{13}) and control (Ω_{23}) microwave fields which satisfy Eq. (3) would result in no population loss through the readout state $|3\rangle$. In this way, S-EIT would confirm, without disturbing the system, that we had indeed prepared the qubit in the desired state.

In a practical SQC, there will be decoherence of the state $|\Psi\rangle$, and this must be measured, characterized, and minimized for quantum information applications. S-EIT is one such sensitive decoherence probe, since deviations in the amplitude and/or relative phase of the complex coefficients c_i from the condition established in Eq. (3) result in a small probability $|(c_1\Omega_{13} + c_2\Omega_{23})/\Omega|^2$ of the SQC being driven into the readout state $|3\rangle$ on a time scale $\sim \Gamma_3/\Omega^2$. In general, there are two categories of decoherence: *loss* and *dephasing*. *Loss* refers to population losses from the metastable states $|1\rangle, |2\rangle$, and it is present in an SQC due to, for example, the finite loss rate of level $|2\rangle$, $\Gamma_2 \sim 1/\mu\text{s} = (2\pi) 0.2 \text{ MHz}$. *Dephasing* refers to interactions of the SQC with other degrees of the freedom in the system that cause the relative phase between c_1 and c_2 to diffuse. The incorporation of dephasing is facilitated by the use of a density matrix formalism.

We describe the system with a 3×3 density matrix with diagonal elements ρ_{ii} describing the populations, and ρ_{ij} , $i \neq j$ describing the coherences between levels. In the presence of the EIT fields Ω_{13} and Ω_{23} with no direct coupling ($\Omega_{12} = 0$), the Bloch equations govern the evolution of the density matrix [21]:

$$\dot{\rho}_{11} = -\Gamma_1\rho_{11} - \frac{i}{2}\Omega_{13}^*\rho_{31} + \frac{i}{2}\Omega_{13}\rho_{13}, \quad (4)$$

$$\dot{\rho}_{22} = -\Gamma_2\rho_{22} - \frac{i}{2}\Omega_{23}^*\rho_{32} + \frac{i}{2}\Omega_{23}\rho_{23}, \quad (5)$$

$$\begin{aligned} \dot{\rho}_{33} = & -\Gamma_3\rho_{33} + \frac{i}{2}\Omega_{13}^*\rho_{31} - \frac{i}{2}\Omega_{13}\rho_{13} \\ & + \frac{i}{2}\Omega_{23}^*\rho_{32} - \frac{i}{2}\Omega_{23}\rho_{23}, \end{aligned} \quad (6)$$

$$\dot{\rho}_{12} = -\gamma_{12}\rho_{12} - \frac{i}{2}\Omega_{13}^*\rho_{32} + \frac{i}{2}\Omega_{23}\rho_{13}, \quad (7)$$

$$\dot{\rho}_{13} = -\gamma_{13}\rho_{13} + \frac{i}{2}\Omega_{13}^*(\rho_{11} - \rho_{33}) + \frac{i}{2}\Omega_{23}^*\rho_{12}, \quad (8)$$

$$\dot{\rho}_{23} = -\gamma_{23}\rho_{23} + \frac{i}{2}\Omega_{23}^*(\rho_{22} - \rho_{33}) + \frac{i}{2}\Omega_{13}^*\rho_{21}. \quad (9)$$

The remaining three elements' equations are determined by $\rho_{ij}^* = \rho_{ji}$. The decoherence rates $\gamma_{ij} = (\Gamma_i + \Gamma_j)/2 + \gamma_{ij}^{(\text{deph})}$ include both loss and dephasing contributions. We concentrate on the regime in which the readout state escape rate $\Gamma_3 = 1 \text{ ns}^{-1} = (2\pi) 130 \text{ MHz}$ dominates all other loss and dephasing rates, thus $\gamma_{13} \approx \gamma_{23} \approx \Gamma_3/2$. Furthermore, we ignore the meta-stable state losses Γ_1, Γ_2 relative to the dephasing $\gamma_{12}^{(\text{deph})}$ and set $\gamma_{12} \approx \gamma_{12}^{(\text{deph})}$. Theoretical estimates of dephasing rates, such as $\gamma_{12}^{(\text{deph})}$, in multi-level systems were recently obtained in Ref. 23.

We illustrate an S-EIT decoherence probe example by applying EIT fields $\Omega_{13} = \Omega_{23} = (2\pi) 150 \text{ MHz}$ to the dark state $|\Psi\rangle = (|1\rangle - |2\rangle)/\sqrt{2}$ with a dephasing rate $\gamma_{12} = (2\pi) 5 \text{ MHz}$ and numerically integrating Eqs. (4)-(9). The dephasing γ_{12} causes a small population transfer to the excited state ρ_{33} (Fig. 2a). The excited state population initially exhibits a rapid rise (see inset Fig. 2a)

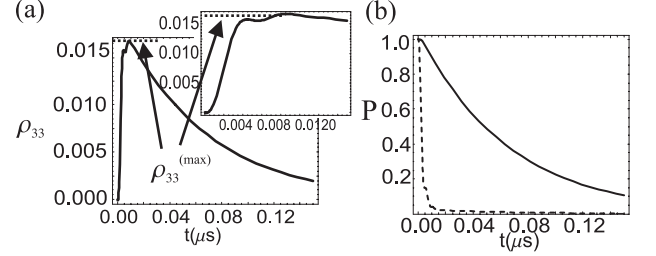


FIG. 2: (a) The population (occupation probability) ρ_{33} as a function of time with EIT fields $\Omega_{13} = \Omega_{23} = (2\pi) 150 \text{ MHz}$ applied to an initial dark state $\rho_{11} = \rho_{22} = 0.5$ and $\rho_{12} = -0.5$, and with a dephasing rate $\gamma_{12} = (2\pi) 5 \text{ MHz}$. The inset shows the same curve zoomed in on the early times. Under conditions of good EIT, we see a rapid initial rise to some plateau, followed by a much slower decay. (b) The total population $P(t)$ remaining in the system versus time for the same simulation (solid curve). For comparison, the dashed curve shows the population for the out of phase case $\rho_{11} = \rho_{22} = 0.5$ and $\rho_{12} = 0.5$ discussed in the text.

with transitory oscillations, reaching its maximum value $\rho_{33}^{(\text{max})}$ within about 4 ns. This is followed by a smooth decay with a $1/e$ time of about 80 ns. The solid curve in Fig. 2b traces the total population $P = \rho_{11} + \rho_{22} + \rho_{33}$ remaining in the system as a function of time. When the excited state maximum $\rho_{33}^{(\text{max})}$ is reached, the total remaining population is $P(4 \text{ ns}) = 0.973$. In contrast, the dashed line in Fig. 2b illustrates the rapid population loss expected when the same fields are applied to the state $|\Psi\rangle = (|1\rangle + |2\rangle)/\sqrt{2}$ [π out of phase with the dark state in Eq. (3)]. In the absence of S-EIT quantum interference, the entire population is lost on a time scale $\Gamma_3/\Omega^2 \sim 1 \text{ ns}$. The general behavior presented in Figs. 2a and 2b is observed over a wide parameter regime of experimental interest.

We now use Eqs. (4)-(9) to show how measuring the slow population loss in S-EIT can be used to extract the decoherence rate γ_{12} . The elements ρ_{33} , ρ_{13} , and ρ_{23} in Eqs. 6, 8, and 9 are damped at a rapid rate $\sim \Gamma_3$, allowing their adiabatic elimination [22, 24]; we solve for their quasi-steady state values by setting $\dot{\rho}_{33} = \dot{\rho}_{13} = \dot{\rho}_{23} = 0$. This approximation is accurate once initial transients have passed and the plateau value $\rho_{33}^{(\text{max})}$ has been reached. Using these results in Eq. (7) yields an equation for $\dot{\rho}_{12}$ with a strong damping term Ω^2/Γ_3 , and it too can be solved for its quasi-steady state value. In the limit $\gamma_{12}\Gamma_3/\Omega^2 \ll 1$ we get [25]

$$\rho_{12}(t) \approx -\frac{\Omega_{13}\Omega_{23}}{\Omega^2} \left(1 - \frac{2\gamma_{12}\Gamma_3}{\Omega^2} \right) (\rho_{11}(t) + \rho_{22}(t)). \quad (10)$$

The ratio $2\gamma_{12}\Gamma_3/\Omega^2$ represents the small fractional deviation of ρ_{12} from its dark state value. There is a competition between the “preparation rate” Ω^2/Γ_3 (which constantly acts to drive the system into the dark state) and the decoherence rate γ_{12} (which attempts to drive it back out).

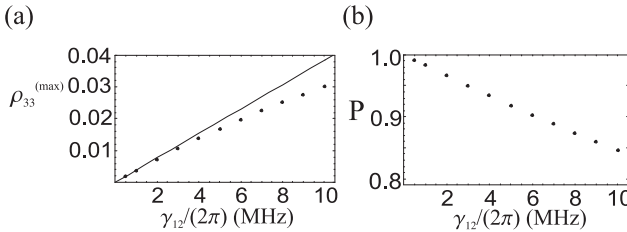


FIG. 3: (a) The maximum plateau value $\rho_{33}^{(\max)}$ for different γ_{12} (circles). The solid curve shows the prediction (11). (b) The remaining population $P = \rho_{11} + \rho_{22} + \rho_{33}$ at the time the plateau is reached for the cases in (a).

We now consider the conditions under which one can use S-EIT to estimate the decoherence rate with little population loss in the system. Eqs. (4), (5), and (10) reveal that deviations from the dark state cause population loss through $|3\rangle$ at a rate $R = 2\gamma_{12}(\Omega_{13}^2\Omega_{23}^2/\Omega^4)$; this ultimately leads to the exponential decay of P seen in Fig. 2b. By assumption, population escapes the system only through the decay term $-\rho_{33}\Gamma_3$ in Eq. (6), yielding $\rho_{33} = (R/\Gamma_3)P$. At the early time when $\rho_{33}^{(\max)}$ has been reached, the population P remains close to unity, and the excited state population reaches

$$\rho_{33}^{(\max)} \approx 2 \frac{\Omega_{13}^2 \Omega_{23}^2}{\Omega^4} \frac{\gamma_{12}}{\Gamma_3}. \quad (11)$$

The time T_{ss} to reach $\rho_{33}^{(\max)}$ is generally the smaller of the preparation time $\sim \Gamma_3/\Omega^2$ and the inverse of the decay rate $1/\Gamma_3$. At this time, the total population loss will be $\sim T_{ss}\rho_{33}^{(\max)} \sim (2\Omega_{13}^2\Omega_{23}^2/\Omega^4) \text{Max}(\gamma_{12}/\Gamma_3, \gamma_{12}\Gamma_3/\Omega^2)$. So long as the loss during this initial transient time is small, the population will follow a simple exponential decay $P(t) = \exp(-\rho_{33}^{(\max)}\Gamma_3 t)$, and the dephasing rate γ_{12} can be easily extracted. To keep this loss small, we require both ratios in the $\text{Max}(\dots)$ argument to be small ($\Omega \gg \sqrt{2\gamma_{12}\Gamma_3}$ and $\Gamma_3 \gg \gamma_{12}$) in order to use this approach to accurately estimate the decoherence rate while causing little loss from the system. Since Ω is experimentally controllable, it can be chosen to satisfy the first

constraint. If Γ_3 is comparable or smaller than γ_{12} , then S-EIT remains a decoherence probe, although the strong damping assumption leading to Eq. (10) no longer holds and so the analysis is different.

We have performed a series of numerical simulations, varying γ_{12} to test the validity of the above approach. The results are presented in Fig. 3. Fig. 3a indicates $\rho_{33}^{(\max)}$ versus γ_{12} and compares the results with the analytic estimate [Eq. (11)]. The agreement is quite good for $\gamma_{12} < (2\pi) 4$ MHz, which corresponds to the $2\gamma_{12}\Gamma_3/\Omega^2 < 0.056$. Higher dephasing rates compete more with the preparation rate, making the adiabatic elimination approach less valid; this leads to deviations from our analytic prediction [Eq. (11)]. In such cases, one observes a significant loss by the time $\rho_{33}^{(\max)}$ is reached, as illustrated in Fig. 3b

The RWA invoked in the calculation ignores far off-resonance couplings induced by other applied fields at other transitions (*e.g.*, in our case, the Ω_{23} field drives $|1\rangle \leftrightarrow |2\rangle$ at $\Delta \sim 4$ GHz off resonance). We have performed calculations including all such off-resonant couplings. Generally, they lead to small shifts of the energy levels (analogous to A.C. Stark shifts) and loss rates. These losses scale as $\Gamma_3(\Omega^2/\Delta^2)$ and $\Omega^4/\Gamma_3^2\Delta$, putting a limit on the field strengths Ω^2 which can be used for a given Δ . For the parameters considered here, we found shifts of $(2\pi) 8$ MHz and loss rates totalling $(2\pi) 19$ kHz; this should not effect measurements in the regime $\gamma_{12} \gg (2\pi) 19$ kHz [25].

We have proposed using the superconductive analog to EIT (S-EIT) to demonstrate macroscopic quantum interference in superconductive quantum circuits. S-EIT provides an accurate and sensitive means to probe the accuracy and phase coherence of qubit preparation, and we have calculated analytic expressions for the field strengths required for this purpose.

This work was supported in part by the AFOSR grant No. F49620-01-1-0457 under the Department of Defense University Research Initiative in Nanotechnology (DURINT). The work at Lincoln Laboratory was sponsored by the AFOSR under Air Force Contract No. F19628-00-C-0002.

-
- [1] A. J. Leggett and A. Garg, Phys. Rev. Lett. **54**, 857 (1985).
[2] Y. Nakamura, Y. A. Pashkin, and J. S. Tsai, Nature **398**, 786 (1999).
[3] J. R. Friedman, *et al.*, Nature **406**, 43 (2000).
[4] C. H. van der Wal, *et al.*, Science **290**, 773 (2000).
[5] D. Vion, *et al.*, Science **296**, 886 (2002).
[6] Y. Yu, *et al.*, Science **296**, 889 (2002).
[7] J. M. Martinis, S. Nam, J. Aumentado, and C. Urbina, Phys. Rev. Lett. **89**, 117901 (2002).
[8] I. Chiorescu, *et al.*, Science **299**, 1869 (2003).
[9] Y. A. Pashkin, *et al.*, Nature **421**, 823 (2003).
[10] K. J. Boller, A. Imamoglu, and S. E. Harris, Phys. Rev. Lett. **66**, 2593 (1991).
[11] S. E. Harris, Phys. Today **50**, 36 (1997).
[12] J. Ruostekoski and D. F. Walls, Phys. Rev. A, **59** R2571 (1999).
[13] L. V. Hau, S. E. Harris, Z. Dutton, and C. H. Behroozi, Nature **397**, 594 (1999).
[14] M. M. Kash, *et al.*, Phys. Rev. Lett. **82**, 5229 (1999).
[15] D. Budker, D. F. Kimball, S. M. Rochester, and V. V. Yashchuk, Phys. Rev. Lett. **83**, 1767 (1999).
[16] K. Segall, *et al.*, Phys. Rev. B **67**, 220506 (2003).
[17] Y. Yu, *et al.*, submitted to PRL (2003).
[18] D. S. Crankshaw, *et al.*, submitted to PRB (2003).
[19] T. P. Orlando, *et al.*, Phys. Rev. B **60**, 15398 (1999).

- [20] J. E. Mooij, *et al.*, *Science* **285**, 1036 (1999).
- [21] M. O. Scully and M. S. Zubairy, *Quantum Optics*, Cambridge Univ. Press, Cambridge (1997).
- [22] Z. Dutton, Ph.D. thesis, Harvard University (2002).
- [23] G. Burkard, R. H. Koch, and D. P. DiVincenzo, cond-mat/0308025.
- [24] J. Javanainen and J. Ruostekoski, *Phys. Rev. A*, **52** 3033 (1995).
- [25] K. V. R. M. Murali, D. Crankshaw, T. P. Orlando, Z. Dutton, and W. D. Oliver, *in preparation*.